Aalborg Universitet

AALBORG UNIVERSITY

Decentralized Method for Load Sharing and Power Management in a PV/Battery Hybrid Source Islanded Microgrid

Karimi, Yaser; Oraee, Hashem; Golsorkhi, Mohammad; Guerrero, Josep M.

Decentralized Method for Load Sharing and Power Management in a PV/Battery Hybrid Source Islanded Microgrid

Yaser Karimi, Hashem Oraee, *Senior Member, IEEE,* Mohammad S. Golsorkhi, *Graduate Student Member, IEEE*, Josep M. Guerrero, *Fellow, IEEE*

Abstract— **This paper proposes a new decentralized power management and load sharing method for a photovoltaic based islanded microgrid consisting of various PV units, battery units and hybrid PV/battery units. Unlike the previous methods in the literature, there is no need to communication among the units and the proposed method is not limited to the systems with separate PV and battery units or systems with only one hybrid unit. The proposed method takes into account the available PV power and battery conditions of the units to share the load among them. To cover all possible conditions of the microgrid, the operation of each unit is divided into five states and modified active power-frequency droop functions are used according to operating states. The frequency level is used as trigger for switching between the states. Efficacy of the proposed method in different load, PV generation and battery conditions is validated experimentally in a microgrid lab prototype consisted of three units.**

Index Terms— **decentralized power management; hybrid source microgrid; hybrid PV/battery unit; SoC; PV power curtailment;**

I. INTRODUCTION

D ue to environmental concerns and continuous decrease in the price, photovoltaic (PV) generations have been increasing in the recent years [1, 2]. The intermittency of PV generations necessitates the integration of battery storage in the grid [3]. The combination of PVs, battery storages and loads can form a microgrid (MG). When the grid is present, the MG operates in grid-connected mode to exchange power with the main utility, and the battery storage can perform different roles such as frequency control, instantaneous reserve, and peak shaving [4, 5] . If a disturbance occurs in the main utility, the MG can be disconnected to operate in islanded mode [6] .

Battery storage can be connected as a separate unit to the MG or can be combined with the PV unit forming a hybrid source unit [5, 7, 8]. While both configurations are widely used, the latter is more cost effective because the direct charging of the battery from the PV increases efficiency; moreover, the use of

a single inverter for the PV and battery reduces the cost of components.

In islanded mode of operation, the control system objectives are sharing the load among different units and balancing the power in the MG while considering power rating and PV generation of the units and State of Charge (SoC) of the batteries [9]. These objectives can be achieved by centralized [10-12] or decentralized [7, 13-18] power management. The centralized control strategies rely on communication among units and loads in the MG, which reduces the reliability of the system [16, 19]. The decentralized control methods, however, only require local measurements. In addition, non-crucial communication can be used along with the decentralized control to achieve other objectives such as restoring voltage and frequency deviations [20, 21]. Several decentralized control strategies for power management of islanded MGs consisting of distributed generations (DGs) and batteries have been proposed in the literature. In [13-15] frequency signaling technique is utilized for the power management. However, the applications of these methods are limited to the MGs composed of only one energy storage unit. In [16] a frequency based energy management strategy is proposed for a MG with distributed battery storage but it is only valid for systems with separate battery units; moreover, in some modes it transfers power from some of the batteries to the others, which reduces the overall efficiency of the system because of the power losses during charging and discharging of the batteries. Similarly, the frequency bus-signaling method proposed in [17] is only applicable to separate battery units. In [18], separate battery storage and PV units are controlled based on modified droop method, whereas in [7] the method is adapted for a single hybrid unit connected to a droop controlled MG. However, those methods are not applicable to the MGs consisting of multiple hybrid units.

This paper proposes a decentralized method for power management and load sharing in an islanded MG consisting of different PV units, battery storage units and hybrid PV/battery units. Unlike previous works, the proposed method is not limited to the systems with separate PV and battery units or systems with only one hybrid unit. In the proposed method, the MG can be in three modes and the operation of each unit in the MG is divided into five states according to load, PV generation and battery conditions. To achieve the decentralized power management, conventional active power-frequency (*P-f*) droop function [6, 22-24] is modified according to each state;

Y. Karimi and H. Oraee are with the Department of Electrical Engineering, Sharif University of Technology, Tehran, Iran.(emails: y_karimi@ee.sharif.edu, oraee@sharif.edu).

M.S. Golsorkhi is with the School of Electrical and Information Engineering, University of Sydney, NSW2006, Australia (email: mohammad.golsorkhiesfahani@sydney.edu.au).

J. M. Guerrero is with the Department of Energy Technology, Aalborg University, 9220 Aalborg East, Denmark (e-mail: joz@et.aau.dk).

moreover, the frequency level is used to trigger state changes in each unit. The proposed method has the following features and the contribution of the paper is providing them without relying on any communications or central management system.

• It provides power management for MGs consisting of PV, battery and hybrid PV/battery units.

• When the total load is more than total PV generation, all PV sources (in both separate and hybrid units) operate in Maximum Power Point (MPP) and all the batteries (in both separate and hybrid units) supply the surplus load power. The surplus power is shared among the batteries so that batteries with higher SoC have higher discharging power.

• In case that the total PV generation is more than total load and the batteries in the MG have the capacity to absorb the surplus power, the batteries are charged with the excess PV power. The excess power is shared among the batteries so that batteries with lower SoC absorb more power. In addition, each battery can be charged with PV power of other units.

• When the total PV generation is more than total load and all batteries are completely charged or reach their maximum charging power, PV power curtailment is performed and load is shared among the units that have PV source based on the inverter capacity and considering their available PV power.

• In all operating modes, the SoC and charging power limits of batteries and the power rating of the units are respected.

It is worth noting that the proposed method is applicable to both single-phase and three-phase MGs but for simplicity, single-phase MG is considered in this paper. Moreover, other sources other than PV can be used in the units.

The rest of the paper is organized as follows: in section II the general structure of the hybrid source single-phase MG is presented. In section III the proposed method is presented in detail and operating modes of the whole MG, different load sharing strategies, operating states of each unit in the MG and criteria for changing the states are presented. The proposed method is validated experimentally in section IV. Section V concludes the paper.

II. Single-Phase Microgrid Structure

A typical single-phase MG consisting of PV, battery and hybrid source units is depicted in Fig. 1. With the intention of being comprehensive, a MG with only hybrid units is considered in the following analysis. The proposed method can be easily applied to separate PV and battery units with minor changes. Each hybrid unit consists of a single-phase inverter connected to the Point of Common Coupling (PCC) through a LCL filter, a PV array connected to the dc-link via a dc-dc boost converter and a battery storage connected to the dc-link via a bidirectional dc-dc boost converter. All the MG loads are centralized in a single load.

By using an inductance in the output filter of each unit and by implementing virtual inductance [25, 26], it is ensured that the output impedance of units is mainly inductive. Therefore, the modified *P-f* droop functions which will be described in the next section along with the conventional *Q-E* droop can be applied for active and reactive power sharing, respectively.

Fig. 2 shows the structure of the proposed control strategy for the inverter part of the unit. Control of the dc-dc converters are
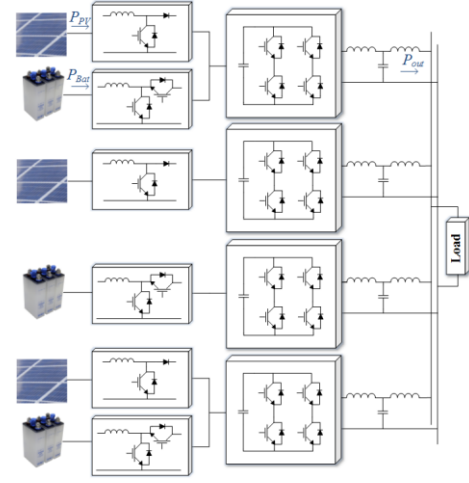

Fig. 1. Typical single-phase microgrid structure

well described in [7, 15, 27]. In the inverter control system, Power Calculation block measures the output active and reactive powers using the method proposed in [28] for single-phase inverters. The amplitude of output voltage reference is determined by the conventional droop equation,

$$E = E^* - m_q Q_{out} \qquad (1)$$

in which E is the amplitude of output voltage reference, E^* is its nominal value, m_q is the droop coefficient and Q_{out} is the output reactive power. The frequency of the output voltage reference is calculated based on a new frequency signaling method, as detailed in the following section. A virtual impedance (R_v+jL_v) is added using the Virtual Impedance block as described in [29] to decouple the active and reactive power regulations. Proportional-Resonant (PR) controller [23] is used for inner voltage and current control loops to track the reference voltage.

III. Proposed Power Management Method

In this section, the details of the decentralized control strategy for power management and load sharing in a hybrid source single-phase MG are discussed. It is worth mentioning that this method can be similarly applied to three-phase MGs.

Note that this paper is only focused on active power sharing and reactive power sharing is out of scope of the paper. First, the general operating modes of the whole MG are presented; then, the operating states of each hybrid unit and criteria for changing of the states are described.

A. The Microgrid Operating Modes

Depending on the load, maximum available PV power and charging capacity of the batteries, the MG can operate in three main modes. In order to achieve the decentralized power management and load sharing, the following general droop function is modified according to MG operating mode to determine output voltage frequency, *f*.

$$f = f_0 + (m_p + \frac{m_i}{s})(P_{ref} - P_{out}) \qquad (2)$$

where f_0 is the nominal frequency of the MG, P_{out} is the output power of the unit, m_p, m_i and P_{ref}, that are determined according to operating mode, are proportional and integral droop coefficients and power reference value, respectively.
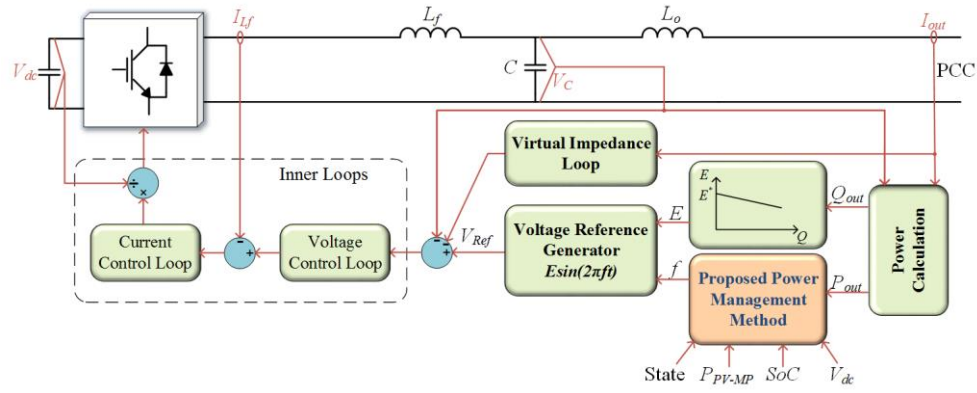
Fig. 2. Control structure of the inverter part of each unit

Mode I)

In this mode, the MG load is larger than total PV maximum power and the batteries in the MG supply the surplus load power. In order to share the surplus load power among the units, three different strategies can be applied.

In the first strategy, the load power is shared among units by means of the conventional P-f droop method. The values of m_p, m_i and P_{ref} for this strategy are selected as:

$$m_p = \frac{\Delta f_{max}}{P_{out-max}} \ , \ m_i = 0 \ , \ P_{ref} = 0 \tag{3}$$

where $P_{out-max}$ is the unit output power limit. In this strategy, the power is shared among the units solely based on the power rating, regardless of the PV maximum power of the units. This strategy has the advantage of even sharing of the power losses among the units. However, it requires PV power curtailment in case the sum of output power and battery charging power capacity of a unit is less than available PV power. Therefore, PV power is not utilized completely with this strategy.

In the second strategy, the PV boost converters in all units are controlled to track the maximum power of PV arrays, and load is shared among the units such that the total discharging power of the batteries is shared among the units based on the SoC of the corresponding battery. The battery keeps the power balance in the dc-link, i.e., generates the difference between the PV and output powers. The P-f droop function parameters in this strategy are as follows, in which, to achieve SoC balancing, the droop coefficient is adaptively updated based on the SoC, similar to method proposed in [30, 31] for DC MGs. In addition, P_{ref} is chosen equal to P_{PV-MP} of the unit to allow the PV to work in MPP.

$$m_p = m_{pd0} \frac{1}{SoC^n} \ , \ m_i = 0 \ , \ P_{ref} = P_{PV-MP} \tag{4}$$

where P_{PV-MP} is the maximum PV power of the unit, which is dependent on the solar irradiance and temperature of the PV array, m_{pd0} is a constant value that is selected such that the system is stable in the possible range of SoC and n adjusts the SoC balancing speed [30, 31]. Neglecting the converter power losses, the discharging power of the battery is expressed as:

$$P_{Bat} = P_{out} - P_{PV} , \tag{5}$$

therefore, (2), using the parameters of (4), is equal to

$$f = f_0 - m_p P_{Bat} \tag{6}$$

which results in distribution of discharging power according to the SoC. It is worth mentioning that P_{Bat} is positive in

discharging mode and is negative in charging mode.

In the third strategy, in addition to the SoC of unit's battery, the remaining inverter capacity when PV works at maximum power is also considered in load sharing. The P-f droop function parameters for this strategy are:

$$m_p = m_{pd0} \frac{1}{SoC^n} \times \frac{P_{out-max}}{P_{out-max} - P_{V-MP}} \ , \tag{7}$$

$$m_i = 0 \ , \ P_{ref} = P_{PV-MP}$$

With this strategy, if the SoC of all batteries are equal, the discharging power of the unit with higher PV generation is less than the unit with lower PV generation. In this strategy, unlike the first one, all units work at PV maximum power and the output power of the units are more balanced than second strategy.

The choice of the strategy depends on the MG power sharing objectives but usually the first strategy is not acceptable due to less utilization of PV arrays. In this paper the second strategy is selected. However, the third strategy can be applied similarly.

Mode II)

In this mode, the MG load is less than total PV maximum power but the batteries have the capability to absorb the surplus PV power. Therefore, all PVs work at MPP and the batteries are charged with the surplus power. Based on SoC and rating of the batteries, some units may be in charge limiting state to limit charging power of the battery (State 2).

For the units which are not in charge limiting state, V_{dc} is regulated by the battery boost converter, the inverter is in Voltage Control Mode (VCM) and the output power is controlled according to the following P-f droop function parameters:

$$m_p = m_{pc0} SoC^n \ , \ m_i = 0 \ , \ P_{ref} = P_{PV-MP} \tag{8}$$

in which droop coefficient is adjusted proportional to SoC of the battery, similar to method proposed in [31] for DC MGs, so that batteries with higher SoC absorb less power. m_{pc0} is a constant value that is selected such that the system is stable in the possible operating values of SoC.

For the units which are in charge limiting state, the inverter is in Power Control Mode (PCM) and the output power is controlled by the following droop parameters:

$$m_p = K_{P-P}, m_i = K_{P-I}, P_{ref} = (K_{V-P} + \frac{K_{V-I}}{s})(V_{dc} - V_{dc}^*) \tag{9}$$

where V_{dc}^* is the reference value of dc-link voltage, K_{V-P} and K_{V-I} are proportional and integral gains of V_{dc} controller and

K_{P-P} and K_{P-I} are proportional and integral gains of output power controller. In steady-state conditions, neglecting the power losses,

$$P_{ref} = P_{PV-MP} - |P_{ChLimit}|, \qquad (10)$$

where $P_{ChLimit}<0$ is the maximum permissible charging power of the battery which depends on the rating, voltage and charging state of the battery and is zero when battery reaches SoC_{max}. This control strategy enables distributing the charging power among the batteries. So, each battery can be charged with PV power of other units.

Mode III)

In this mode, the sum of MG load and total charging capacity of the batteries is less than total PV maximum power, therefore, in order to keep the power balance, PV power curtailment should be performed in some units. In this mode, all batteries are charged with maximum power, units with insufficient PV maximum power (as described in the following) work at MPP and are controlled in PCM based on (9), units with sufficient PV maximum power are controlled in VCM and PV boost converter controls the dc-link voltage. The conventional *P-f* droop is used for VCM units in this mode and the droop parameters are, as follows:

$$m_p = \frac{\Delta f_{max}}{P_{out-max}} \;,\; m_i = 0 \;,\; P_{ref} = 0 \qquad (11)$$

Assuming slow variation in SoC of the batteries and PV maximum power, the small-signal behavior of the proposed method in both VCM and PCM is similar to conventional droop function. The small-signal analysis of VCM and PCM modes for PV + battery based microgrids is thoroughly carried out in [7] and [17], and is not repeated here for brevity. Using small-signal analysis, the stable range of the droop coefficients are determined and the parameters m_{pd0} and m_{pc0} are selected such that for all possible operating values of SoC, m_p is always in this range.

B. Operating States of Each Unit in the Microgrid

Each unit in the MG can operate in five states: 1. Battery charge-discharge 2. Battery charge limit 3. PV power curtailment 4. Battery disconnect 5. Output power limit

The modes of operation of the inverters and PV and battery boost converters for different states are summarized in Table I. The control strategy in each state and the criteria for transition between the states are detailed in the following:

State 1:

This state corresponds with the normal operation of the unit, i.e., when neither the SoC nor the currents have reached the limits. In this state, the frequency is adjusted according to (4) or (8), depending on the discharging or charging of the battery. Discharging and charging modes of the unit are associated with Mode I and VCM condition of Mode II of the MG operating modes, respectively. In this state, PV works at MPP and battery boost converter regulates V_{dc}.

In case that P_{PV-MP} of the unit is small or zero and the MG is operated in Mode II, P_{out} might be negative, which means that battery is charged with power produced by other units.

➤ The unit can exit the state 1 in case one of the following criteria is met:

TABLE I
OPERATING STATES OF EACH UNIT IN THE MICROGRID

State	1	2	3	4	5
Description	Battery Charge/ Discharge	Battery Charge Limit	PV Power Curtailment	Battery Disconnect	Output Power Limit
Inverter Control	VCM (4) or (8)	PCM (9)	VCM (11)	PCM (9)	PCM (9)
V_{dc} Control	Battery	P_{ref}	PV	P_{ref}	Battery
PV Power	MPP	MPP	<MPP	MPP	MPP

● The battery is completely charged or the battery power reaches the maximum charging power due to decrease in load or increase in PV generation; (i.e., $SoC=SoC_{max}$ or $P_{Bat}=-P_{ChLimit}$ or $I_{Bat}=I_{Bat-max}$ or $V_{Bat} = V_{Bat-max}$). In this case, the state is changed to State 2.

● The SoC reaches to its minimum value, SoC_{min}. In this case, the state is changed to State 4.

● The output power reaches the inverter rating, $P_{out-max}$. In this case, the state is changed to State 5.

State 2:

This state is regarded as the transition state between States 1 and 3. It is a common state in Modes II and III of the MG operating modes in which the unit operates in PCM. The unit enters this state when battery charge limit occurs in State 1 or the unit reaches PV maximum power in State 3. In this state, PV works at MPP, battery is charged with maximum power and V_{dc} is regulated by (9). With this control, the difference between PV power and battery charging power is injected to/absorbed from the MG. Neglecting power losses, the output power of the unit is determined by (10) in steady-state conditions.

➤ The criteria for exiting from State 2 depend on the previous state of the unit and are as follows:

● All units enter this state one by one from State 1 because of load drop, decrease in battery charging power or PV generation rise. In this case, *f* gradually increases due to the integration action in (9) until it saturates to f_{max}. At this point, all units change to State 3 to reduce PV power generation and maintain the power generation/consumption balance.

● When the MG is in Mode II, in which, all units are in State 2 or charging mode of State 1, any increase in load or decrease in PV generation reduces total charging power of the MG. In this case, the imbalance among charging powers of the units is increased because units in State 2 are controlled in constant power and only charging powers of units in State 1 are decreased. To ensure balanced distribution of charging power (with considering SoC of the batteries), each unit that is in State 2 should exit constant power control mode and return to State 1 if its weighted charging power ($m_p/P_{Bat}|$) is higher than the corresponding value of units in State 1. This criterion can be written as,

$$m_{p-i}|P_{Bat-S1-i}| < K_{pm}m_p|P_{Bat}| \qquad (12)$$

$P_{Bat-S1-i}$ is charging power of ith unit that is in State 1 and $K_{pm}<1$ is a margin used for preventing unwanted changing of state because of error in power measurement. Note that according to (8), $m_{p-i}P_{Bat-S1-i}$ are equal for all units in State 1. As P_{Bat} is negative in charging mode, (12) can be written as,

$$m_{p-i}P_{Bat-S1-i} > K_{pm}m_p P_{Bat} \qquad (13)$$

Using (5), (8) and (13), the criterion for returning to State 1 is:

$$f < f_0 - K_{pm} m_p P_{Bat} \quad \text{and} \quad \text{preState} = 1. \tag{14}$$

When this criterion is met and unit returns to State 1, charging power of the unit is determined based on (8) and the unit will no longer enter charge limiting mode. In the case that the unit is in SoC_{max} and $P_{Bat} = 0$, if $f < f_0$ it means that other units are in discharging mode and this unit starts to discharge.

• All units enter this state one by one from State 3 because of increase in load or decrease in PV generation. In this case, f gradually decreases due to the integration action in (9) until it saturates to f_{min}. At this point, all units change to State 1 in order to reduce the battery charging power or enter battery discharging mode.

• When the MG is in Mode III in which all units are in State 3 or State 2, any decrease in load or battery charging power reduces the required PV generation in the MG. In this case, since units in State 2 are controlled in MPP, PV generation of units in State 3 are decreased which increases the uneven distribution of output power and PV generation among the units. To overcome this, each unit in State 2 should return to State 3 if its weighted output power ($m_p P_{out}$) is higher than the corresponding value of the units in State 3. This criterion can be written as,

$$m_{p-i} P_{out-S3-i} < K_{pm} m_p P_{out}, \tag{15}$$

where $P_{out-S3-i}$ is the output power of ith unit that is in State 3. Note that in State 2, P_{out} is equal to P_{ref} determined by (10) in steady-state; furthermore, according to (11), $m_{p-i} P_{out-S3-i}$ are equal for all units in State 3. Using (11) and (15) the criterion for returning to State 3 is:

$$f > f_0 - K_{pm} m_p P_{out} \quad \text{and} \quad \text{preState} = 3. \tag{16}$$

When this criterion is met and the unit returns to State 3, its output power is determined based on (11) and the unit will no longer enter State 2 because of insufficient PV power.

State 3:

This state is associated with Mode III of the MG operating modes in which total PV maximum power is more than total power required by load and charging of the batteries. In this state, the unit's battery is charged with maximum power, output power is controlled by (11) and PV boost converter regulates V_{dc}. In this state, PV power, that is the sum of output power and battery charging power, is less than the MPP.

➢ The criterion for exiting from State 3 is as follows:

• The PV maximum power is less than the sum of output power determined by (11) and battery charging power. In this case, the unit is switched to State 2. This can occur due to load rise, PV generation drop or in case that all units enter State 3 from State 2 but PV power is not sufficient for this unit.

State 4:

When SoC of the battery reaches to SoC_{min}, the unit enters this state. In this state, battery is disconnected to prevent damage due to its deep discharging, PV works at MPP and V_{dc} is regulated by (9). Since $P_{Bat} = 0$, in the steady-state,

$$P_{out} = P_{PV-MP}. \tag{17}$$

In case that all the units enter this state and the MG load power is more than the total PV maximum power, f decreases until it reaches the critical minimum frequency. At this point, load shedding is inevitable and some non-critical loads must be
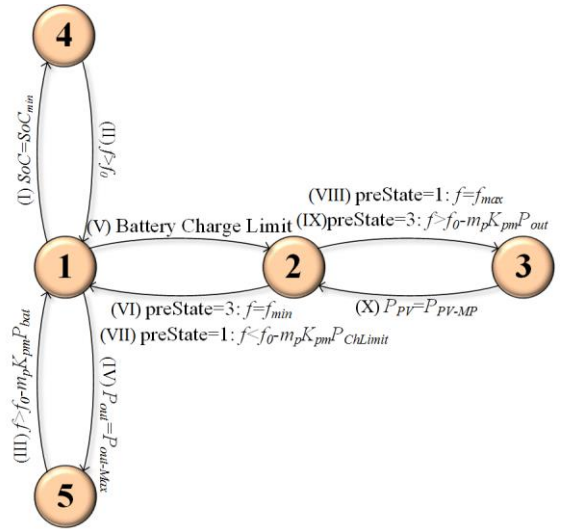

Fig. 3. Criteria for transition between the states of each unit in the MG

disconnected. Load shedding is out of scope of this paper.

➢ The criterion for exiting from State 4 is as follows:

• According to (4) and (8), if $f > f_0$ it indicates that $P_{Bat} < 0$ in units that are in State 1, which means, they are in battery charging mode. At this point, this unit can return to State 1 to charge the battery.

State 5:

When output power of the unit reaches $P_{out-max}$, the unit enters this state to limit its output power. In this state, PV works at MPP and V_{dc} is regulated by the battery boost converter, which controls the battery in discharging mode. The output power is controlled by (9) with $P_{ref} = P_{out-max}$. If all the units enter this state and load power is more than total ratings of the units, f decreases until it reaches the critical minimum frequency. At this point load shedding is inevitable and some non-critical loads must be disconnected.

➢ The criterion for exiting from State 5 is as follows:

• The load is decreased such that the weighted battery discharging power ($m_p P_{Bat}$) of other units in State 1 is less than this unit's corresponding value, i.e.

$$m_{p-i} P_{Bat-S1-i} < K_{pm} m_p P_{Bat}. \tag{18}$$

In this case, the unit can return to State 1. According to (4) and (18), this criterion can be written as,

$$f > f_0 - K_{pm} m_p P_{Bat}. \tag{19}$$

When this criterion is met and the unit returns to State 1, its output power is determined based on (4) and the unit will no longer enter State 5.

The criteria for transition between the states are depicted in Fig. 3. It is worth mentioning that the proposed method does not require an explicit measurement of frequency. The reason is that, during the VCM mode, similar to the conventional droop method, the P-f droop scheme automatically adjusts the frequency of each unit so that all of the units reach a common frequency at steady-state conditions [20]. Also, during the PCM mode of operation, the unit's frequency follows the microgrid frequency due to the integration action in PI controller in (10). Therefore, the unit's frequency is used as f and there is no need to an accurate Frequency Locked Loop (FLL) in order to determine the MG frequency. Fig. 4 illustrates the working
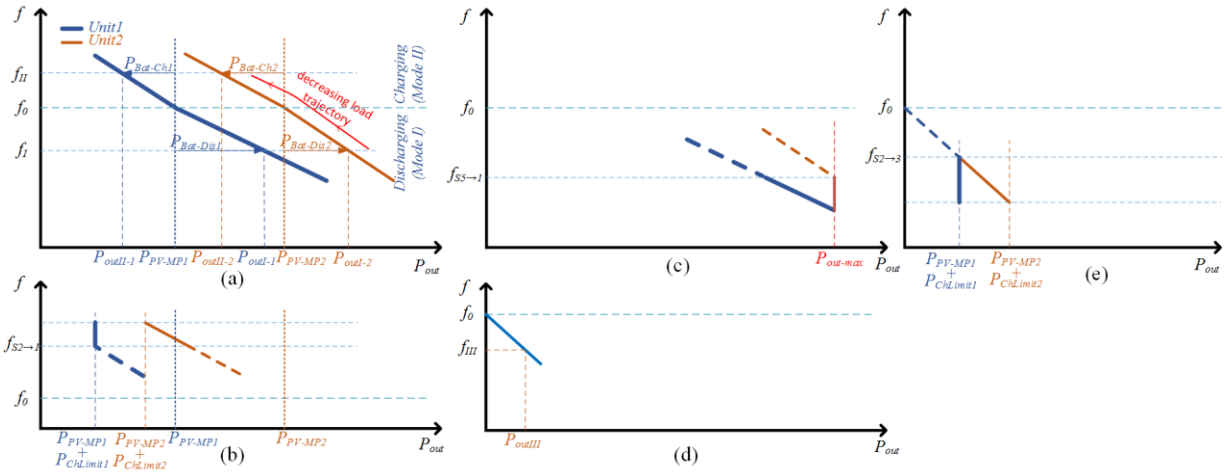
Fig. 4. *P-f* characteristics of a two hybrid unit microgrid
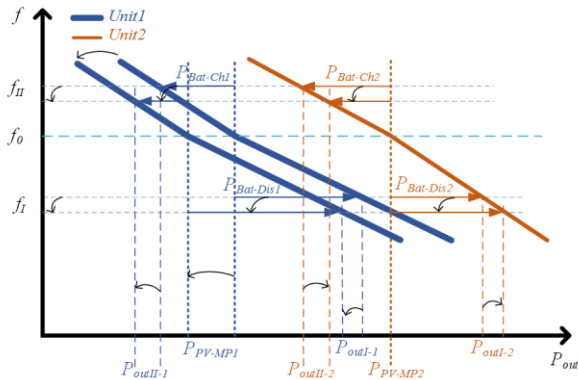
Fig. 5. Shifting the *P-f* characteristic and operating point due to decrease in Unit1 PV maximum power

mechanism and *P-f* characteristics of the proposed method in different states for a MG consisting of two hybrid units. In Fig. 4(a) both units are in normal operation of State 1. Units have PV maximum power as shown in the figure and it is assumed that $SoC_1 > SoC_2$. f_I is a sample operating frequency in a determined load in which the MG is in discharging mode. Due to difference in the slopes of the *P-f* characteristic, the output powers of the units in this frequency (P_{outI-1} and P_{outI-2}) are such that discharging power of Unit1 is higher than Unit2 ($P_{Bat-Dis1} > P_{Bat-Dis2}$). When load is decreased below total PV generation, the MG enters charging mode. f_{II} is a sample operating frequency when the MG is in charging mode and output powers ($P_{outII-1}$ and $P_{outII-2}$) are such that charging power of Unit1 is less than Unit2 ($|P_{Bat-Ch1}| < |P_{Bat-Ch2}|$). With further decrease in the load, charging powers of the units increase. Assuming $|P_{ChLimit1}| < |P_{ChLimit2}|$, Unit1 enters State 2 first. Solid lines in Fig. 4(b) show the case Unit2 is in State 1 and Unit1 is in State 2. Output power of Unit1 is regulated at $P_{PV-MP1} + P_{ChLimit1}$ and Unit2 supplies the remaining load power. Moreover, Unit1 follows the frequency determined by Unit2. Note that, $f_{S2 \rightarrow 1}$ is the frequency in which Unit1 can return to State 1 when load is increased and is equal to criterion (14) with $K_{pm}=1$. On the other hand, in discharging mode, with increase in load power, output powers of both units increase. Because Unit2 has higher P_{PV-MP}, it reaches output power limit first and regulates its output power at $P_{out-max}$. Solid lines in Fig. 4(c) show this case in which Unit1 is in State 1 and Unit2 is in State

5. It is worth noting that, $f_{S5 \rightarrow 1}$ which is equal to criterion (19) with $K_{pm}=1$, is the frequency in which Unit2 can return to State 1 when load is decreased. When the available PV power is more than the sum of MG load and charging power of the batteries, MG works in Mode III. Fig. 4(d), shows the case that both units are in State 3. f_{III} is a sample operating frequency in which both units have equal output powers because they have same m_p. When load is increased, Unit1 reaches maximum PV power and changes to State 2. Solid lines in Fig. 4(e) show the characteristic when Unit1 is in State 2 and Unit2 is in State 3. $f_{S2 \rightarrow 3}$, that is equal to criterion (16) with $K_{pm}=1$, is the frequency in which Unit1 can return to State 3 when load is decreased. Fig. 5 depicts shifting the *P-f* characteristic and operating point due to decrease in Unit1 PV maximum power while keeping the load constant. With decrease in P_{PV-MP1}, the *P-f* characteristic of Unit1 is shifted to the left. Because of PV generation drop, discharging powers of both units are increased and charging powers of both units are decreased.

C. Smooth Transition Between the States

In order to ensure stable operation during state transitions, and prevent transient overcurrent stresses, three smoothing mechanisms are deployed. First of all, the droop coefficients m_p and m_i are passed through a low-pass filter (LPF) with cut-off frequency much smaller than the bandwidth of the droop controller. Secondly, during transition from the PCM to VCM, including changing from State 2 to State 1 (criterion (VI) Fig. 3) and changing from State 2 to State 3 (criterion (VIII)), the reference power, P_{ref} , is passed through a LPF to prevent abrupt frequency changes. Thirdly, to prevent possible transient overcurrent, a protective virtual impedance (resisitive+inductive) is added [32] during the state transitions. The protective virtual impedance is selected such that the unit output voltage does not fall below the permissible range. In addition to protection against overcurrent, the resistive part of the virtual impedance increases system damping [33] and helps the system to reach its new steady-state conditions rapidly. With the intention of improving the voltage regulation, the protective virtual impedance is changed back to zero after the transition.

A. *Modifications for Separate PV and Battery Units*

The case of a separate battery unit is similar with a hybrid unit with no PV generation. So, P_{PV-MP}=0 and State 3 does not exist. In this case, when criterion (VIII) in Fig. 3 is satisfied, the unit remains at State 2 but preState, which indicates the previous state of the unit and is used in selection between criteria (VI) or (VII), is set to 3. In case of separate PV units, assuming PV boost converter limits PV power to the inverter rating, the unit can only operate in States 2 and 3 with $P_{ChLimit}$=0. In this case, when criterion (VI) occurs, the unit remains at State 2 but preState, which is used in selection between criteria (VIII) or (IX), is set to 1.
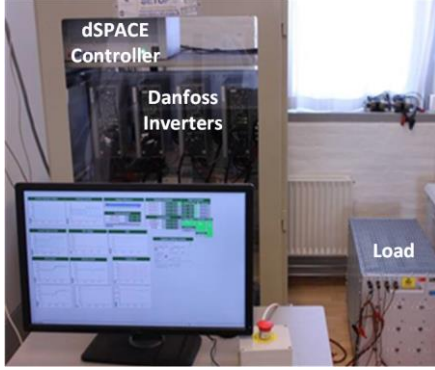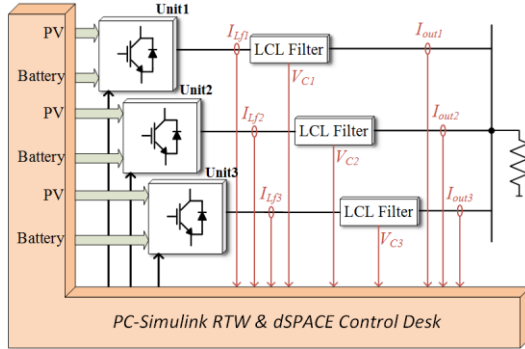

Fig. 6. Experimental setup

Fig. 7. Schematic of the experimental setup

IV. EXPERIMENTAL RESULTS

The proposed method has been evaluated experimentally using the experimental setup shown in Fig. 6 with schematic as shown in Fig. 7. It consists of three Danfoss inverters used as single-phase inverters, a real-time dSPACE1006 platform, LCL filters and load. Batteries and PVs are modeled in MATLAB and emulated in the dSPACE controller. The experimental setup and controller parameters are listed in Table II. The droop coefficients are selected according to small-signal analysis presented in [17]. Based on this analysis, $0.0001 < m_p < 0.04$ and $0 \le m_i < 0.04$ ensure stability in all states.

Assuming $0.65 < SoC < 0.95$ and n=15, choosing m_{pd0}= 0.000047 and m_{pc0}=0.064 guarantees the stability in both charging and discharging modes.

Several experiments are performed to evaluate the performance of the proposed method in different possible conditions of the MG. In the first experiment, the response of the system to load and PV generation variations while the units

TABLE II
EXPERIMENTAL SETUP AND CONTROLLER PARAMETERS

Parameter	Symbol	Value	Unit
Nominal voltage	E^*	220	V_{rms}
Nominal frequency	f_0	50	Hz
Inverter rating	$P_{out-max}$	750	W
Converter side inductance	L_f	3.6	mH
Filter capacitance	C	18	uF
Grid side inductance	L_o	3.6	mH
Virtual inductance	L_v	4	mH
Virtual resistance	R_v	1	Ω
Voltage loop PR	K_{pV}, K_{iV}	0.02, 15	-, S^{-1}
Current loop PR	K_{pI}, K_{iI}	10, 8000	-, S^{-1}
Voltage droop coefficient	m_q	0.007	V/Var
PCM PI controller	K_{P-P}, K_{P-I}	0.0016, 0.008	rad/(W.s), rad/(W.s^2)
SoC balancing	m_{pd0}, m_{pc0}, n	0.000047, 0.064, 15	-

operate in states 1-3, is studied. Other experiments evaluate performance of the system in step load change, output power limiting and SoC balancing in discharging and charging modes. In all experiments, K_{pm}=0.8.

Fig. 8 shows the state, output power, PV power, battery power and output frequency of each unit in different load, PV generation and battery conditions. For clarity of the results in this experiment, m_p is considered independent of the SoC and is equal for all units. The P_{PV-MP} of Units 1, 2 and 3 are considered 300W, 500W and 600W, respectively and the $|P_{ChLimit}|$ of the units are considered 400W, 300W and 150W, respectively. Initially, all the units are in State 1 and load power (which is 1700W) is shared among units according to (4) such that the battery discharging powers of all units are equal. All PVs work at MPP in this state. At t=20s, the load is decreased to 1400W, therefore the discharging power of all batteries are decreased to 5W. At t=40s, the load is decreased to 1100W and since the total PV generation is more than the load, all batteries enter the charging mode with equal charging powers determined by (8). At t=60s, the load is decreased to 800W. As a result, Unit3 that has the minimum $|P_{ChLimit}|$, reaches the maximum charging power and changes to State 2 with output power regulated to $P_{PV-MP}+P_{ChLimit}$. The remaining charging power is equally shared between Units 1 and 2. At t=80s, load is decreased to 500W. Increase in charging power is such that both Units 1 and 2 reach their maximum charging power and change to State 2. Since all units are in State 2, frequency increases until saturates at f_{max}. At this point, all units change to State 3. However, since PV power is not sufficient for supplying both battery charging power and output power determined by (11) in Units 1 and 2, they return to State 2. It is observed that the output power of Unit 1 is negative. This implies that the unit absorbs power from the MG for charging its battery. At t=100s, the load is decreased to 200W. Since Units 1 and 2 are in State 2, regulated to a fixed
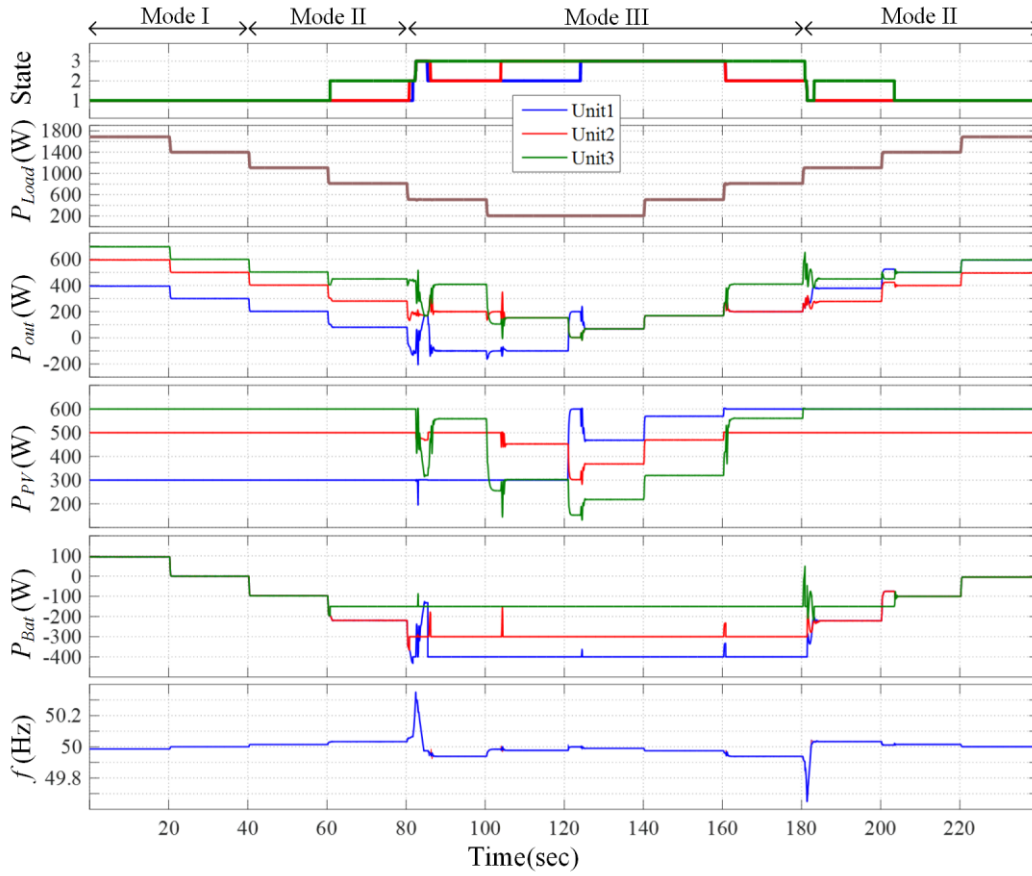
Fig. 8. Experimental results of a three unit single phase microgrid in different load and PV generation conditions

output power, the output power of Unit3 decreases and f increases based on (11). After 3s, criterion (16) is validated in Unit2 and it returns to State 3. As a result, its PV generation drops accordingly.   At t=120s, the irradiance of Unit1 PV is increased leading to increase in its maximum power from 300W to 600W. Consequently, the output power of Unit1 increases to 200W. Since the load power is constant, the output power of Unit3 is decreased and f is increased according to (11). After 3s, criterion (16) is validated in Unit1 and it also returns to State 3. At this point, all units are in State 3. At t=140s, the load is increased to 500W but the units remain at State 3 and the output power of all units increase equally. At t=160s, the load is increased to 800W and Units 1 and 2 reach their maximum PV power and change to State 2. At t=180s, the load is increased to 1100 W. Consequently, Unit3 also reaches its maximum PV power and changes to State 2. Since all units are in State 2, frequency decreases until saturates at f_{min}. At this point, all the units change to State 1. However, since Unit3 battery charging power determined by (8) is more than its maximum value, it returns to State 2. At t=200s, the load is increased to 1400W. The output powers of Units 1 and 2 increase, resulting in decrease in f based on (8). After 3s, Unit3 also changes to State 1 as the criterion (14) is validated. At this point, all units are in State 1 having same battery charging powers. At t=220s, load is increased to 1700W and the charging power of all units decrease equally to -4W.

    Fig. 9 shows the system response to step load change. At t=20s the load is changed from 1650W to 100 W and at t=40s
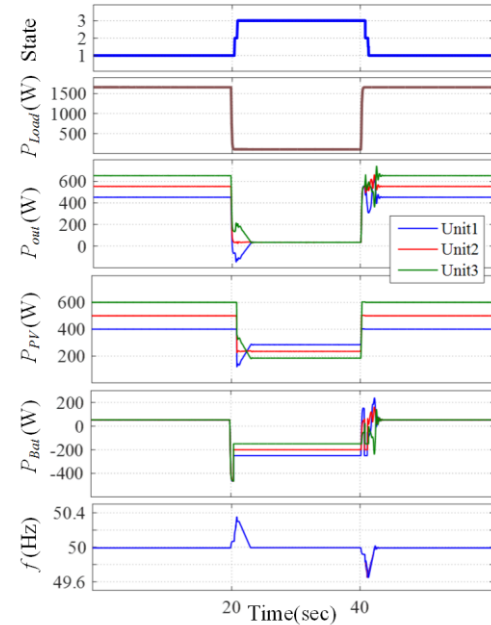

Fig. 9. Step load response

it is returned to 1650W. The proposed method successfully changes the state of all the three units from State 1 to State 3 and then from State 3 to State 1 to cope with the load variations.
    Fig. 10 shows how the units go to output power limiting state. It is assumed that the maximum power of each unit is $P_{out\text{-}max}$=750W. At t=20s, the load is increased from 1600 to 1950W.
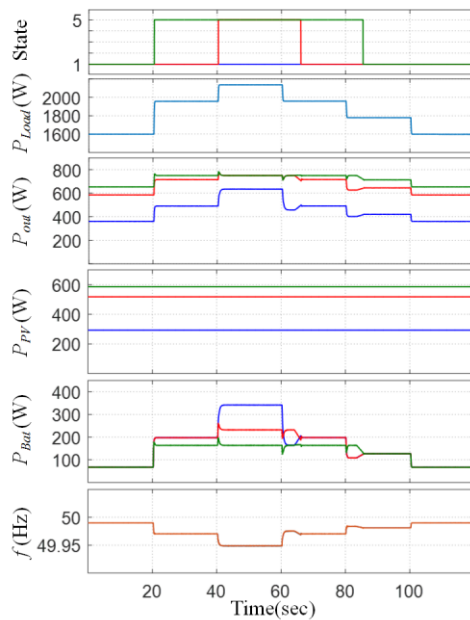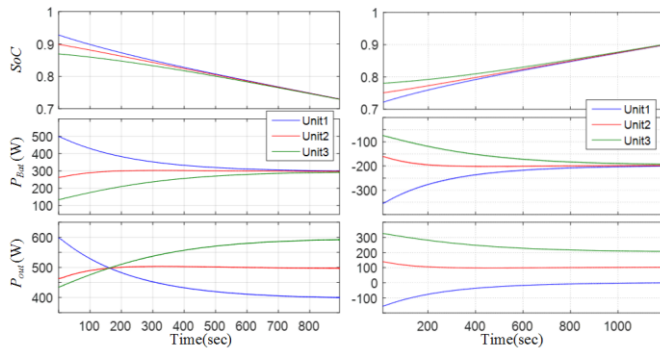
Fig. 10. Output power limiting

Fig. 11. SoC balancing in discharging (left) and charging (right) mode

V. Conclusion

In this paper, a decentralized control method is proposed for power management and load sharing in islanded MGs consisting of PV units, battery units and hybrid PV/battery units. Unlike the previous methods in the literature, the proposed method is not limited to MGs with separate PV and battery units or just one hybrid unit. In this method, the whole MG can operate in three modes and the operation of each unit in the MG is divided into five states according to load, PV generation and battery conditions, in which, frequency level is used as trigger for transition between the states. In each state, specific modified droop function is used for output power control and dc-link is regulated by PV boost converter, battery boost converter or by regulating output power. Although the proposed method is described for a MG consisting of only hybrid units, it can be easily applied to separate battery and PV units with minor modification. Several experiments are performed to evaluate the performance of the proposed method in different possible conditions of a three hybrid unit MG. The results show that the proposed method can successfully adopt the operating state, output power, PV generation and battery charging power of each unit to the MG operating conditions.

Since Unit3 output power determined by (4) is higher than $P_{out-max}$, it changes to State 5 and limits its output power to 750W. At t=40s the load is increased to 2150W. Subsequently, Unit2 also changes to State 5 and its output power is limited. At t=60s, load is decreased to 1950W resulting in increase in f. After 6s, criterion (19) is validated for Unit2 and it returns to State 1. This condition happens to Unit3 at t=80s after decreasing load to 1600W.

Fig. 11 shows SoC balancing of the batteries in discharging and charging modes. All the units are in State 1 and the powers of the batteries are determined by (4) in discharging and by (8) in charging modes, with n=15. In discharging mode, because of high imbalance between the SoCs, difference between battery discharging powers is high at start and Unit1 which has the highest SoC, discharges with the highest power. The SoCs, and consequently, battery discharging powers gradually converge. In charging mode, Unit1 that has the lowest SoC charges with the highest power at start and finally, SoCs and charging powers converge.

References

[1] Z. Li, S. Kai, X. Yan, and X. Mu, "H6 Transformerless Full-Bridge PV Grid-Tied Inverters," *Power Electronics, IEEE Transactions on,* vol. 29, pp. 1229-1238, 2014.

[2] T. Kerekes, M. Liserre, R. Teodorescu, C. Klumpner, and M. Sumner, "Evaluation of Three-Phase Transformerless Photovoltaic Inverter Topologies," *Power Electronics, IEEE Transactions on,* vol. 24, pp. 2202-2211, 2009.

[3] T. Dragicevic, J. M. Guerrero, J. C. Vasquez, and D. Skrlec, "Supervisory Control of an Adaptive-Droop Regulated DC Microgrid With Battery Management Capability," *Power Electronics, IEEE Transactions on,* vol. 29, pp. 695-706, 2014.

[4] I. Serban and C. Marinescu, "Control Strategy of Three-Phase Battery Energy Storage Systems for Frequency Support in Microgrids and with Uninterrupted Supply of Local Loads," *Power Electronics, IEEE Transactions on,* vol. 29, pp. 5010-5020, 2014.

[5] H. Fakham, L. Di, and B. Francois, "Power Control Design of a Battery Charger in a Hybrid Active PV Generator for Load-Following Applications," *Industrial Electronics, IEEE Transactions on,* vol. 58, pp. 85-94, 2011.

[6] J. M. Guerrero, J. C. Vasquez, J. Matas, M. Castilla, and L. G. de Vicuna, "Control Strategy for Flexible Microgrid Based on Parallel Line-Interactive UPS Systems," *Industrial Electronics, IEEE Transactions on,* vol. 56, pp. 726-736, 2009.

[7] H. Mahmood, D. Michaelson, and J. Jin, "Decentralized Power Management of a PV/Battery Hybrid Unit in a Droop-Controlled Islanded Microgrid," *Power Electronics, IEEE Transactions on,* vol. 30, pp. 7215-7229, 2015.

[8] M. Hamzeh, A. Ghazanfari, H. Mokhtari, and H. Karimi, "Integrating Hybrid Power Source Into an Islanded MV Microgrid Using CHB Multilevel Inverter Under Unbalanced and Nonlinear Load Conditions," *Energy Conversion, IEEE Transactions on,* vol. 28, pp. 643-651, 2013.

[9] H. Jinwei and L. Yun Wei, "An Enhanced Microgrid Load Demand Sharing Strategy," *Power Electronics, IEEE Transactions on,* vol. 27, pp. 3984-3995, 2012.

[10] K. T. Tan, P. L. So, Y. C. Chu, and M. Z. Q. Chen, "Coordinated Control and Energy Management of Distributed Generation Inverters in a Microgrid," *Power Delivery, IEEE Transactions on,* vol. 28, pp. 704-713, 2013.

[11] K. T. Tan, X. Y. Peng, P. L. So, Y. C. Chu, and M. Z. Q. Chen, "Centralized Control for Parallel Operation of Distributed Generation Inverters in Microgrids," *Smart Grid, IEEE Transactions on,* vol. 3, pp. 1977-1987, 2012.

[12] K. Jong-Yul, J. Jin-Hong, K. Seul-Ki, C. Changhee, P. June Ho, K. Hak-Man, *et al.*, "Cooperative Control Strategy of Energy Storage System and Microsources for Stabilizing the Microgrid during Islanded Operation," *Power Electronics, IEEE Transactions on,* vol. 25, pp. 3037-3048, 2010.

[13] E. Serban and H. Serban, "A Control Strategy for a Distributed Power Generation Microgrid Application With Voltage- and Current-Controlled Source Converter," *Power Electronics, IEEE Transactions on,* vol. 25, pp. 2981-2992, 2010.

[14] W. Dan, T. Fen, T. Dragicevic, J. C. Vasquez, and J. M. Guerrero, "Autonomous Active Power Control for Islanded AC Microgrids With Photovoltaic Generation and Energy Storage System," *Energy Conversion, IEEE Transactions on,* vol. 29, pp. 882-892, 2014.

[15] J. G. de Matos, F. S.F.e Silva, and L. A. de S Ribeiro, "Power Control in AC Isolated Microgrids With Renewable Energy Sources and Energy Storage Systems," *Industrial Electronics, IEEE Transactions on,* vol. 62, pp. 3490-3498, 2015.

[16] A. Urtasun, E. L. Barrios, P. Sanchis, and L. Marroyo, "Frequency-Based Energy-Management Strategy for Stand-Alone Systems With Distributed Battery Storage," *Power Electronics, IEEE Transactions on,* vol. 30, pp. 4794-4808, 2015.

[17] W. Dan, T. Fen, T. Dragicevic, J. C. Vasquez, and J. M. Guerrero, "A Control Architecture to Coordinate Renewable Energy Sources and Energy Storage Systems in Islanded Microgrids," *Smart Grid, IEEE Transactions on,* vol. 6, pp. 1156-1166, 2015.

[18] H. Mahmood, D. Michaelson, and J. Jin, "Strategies for Independent Deployment and Autonomous Control of PV and Battery Units in Islanded Microgrids," *Emerging and Selected Topics in Power Electronics, IEEE Journal of,* vol. 3, pp. 742-755, 2015.

[19] K. De Brabandere, B. Bolsens, J. Van den Keybus, A. Woyte, J. Driesen, R. Belmans, *et al.*, "A voltage and frequency droop control method for parallel inverters," in *Power Electronics Specialists Conference, 2004. PESC 04. 2004 IEEE 35th Annual*, 2004, pp. 2501-2507 Vol.4.

[20] J. M. Guerrero, J. C. Vasquez, J. Matas, V. de, x00F, L. G. a, *et al.*, "Hierarchical Control of Droop-Controlled AC and DC Microgrids;A General Approach Toward Standardization," *Industrial Electronics, IEEE Transactions on,* vol. 58, pp. 158-172, 2011.

[21] Q. Shafiee, J. M. Guerrero, and J. C. Vasquez, "Distributed Secondary Control for Islanded Microgrids;A Novel Approach," *Power Electronics, IEEE Transactions on,* vol. 29, pp. 1018-1031, 2014.

[22] J. M. Guerrero, M. Chandorkar, T. Lee, and P. C. Loh, "Advanced Control Architectures for Intelligent Microgrids; Part I: Decentralized and Hierarchical Control," *Industrial Electronics, IEEE Transactions on,* vol. 60, pp. 1254-1262, 2013.

[23] J. C. Vasquez, J. M. Guerrero, M. Savaghebi, J. Eloy-Garcia, and R. Teodorescu, "Modeling, Analysis, and Design of Stationary-Reference-Frame Droop-Controlled Parallel Three-Phase Voltage Source Inverters," *Industrial Electronics, IEEE Transactions on,* vol. 60, pp. 1271-1280, 2013.

[24] J. M. Guerrero, H. Lijun, and J. Uceda, "Control of Distributed Uninterruptible Power Supply Systems," *Industrial Electronics, IEEE Transactions on,* vol. 55, pp. 2845-2859, 2008.

[25] J. M. Guerrero, L. Garcia De Vicuna, J. Matas, M. Castilla, and J. Miret, "Output Impedance Design of Parallel-Connected UPS Inverters With Wireless Load-Sharing Control," *Industrial Electronics, IEEE Transactions on,* vol. 52, pp. 1126-1135, 2005.

[26] H. Jinwei, L. Yun Wei, J. M. Guerrero, F. Blaabjerg, and J. C. Vasquez, "An Islanding Microgrid Power Sharing Approach Using Enhanced Virtual Impedance Control Scheme," *Power Electronics, IEEE Transactions on,* vol. 28, pp. 5272-5282, 2013.

[27] K. Seul-Ki, J. Jin-Hong, C. Chang-Hee, A. Jong-Bo, and K. Sae-Hyuk, "Dynamic Modeling and Control of a Grid-Connected Hybrid Generation System With Versatile Power Transfer," *Industrial Electronics, IEEE Transactions on,* vol. 55, pp. 1677-1688, 2008.

[28] H. Jinwei, L. Yun Wei, and F. Blaabjerg, "Flexible Microgrid Power Quality Enhancement Using Adaptive Hybrid Voltage and Current Controller," *Industrial Electronics, IEEE Transactions on,* vol. 61, pp. 2784-2794, 2014.

[29] J. Matas, M. Castilla, V. de, x00F, L. G. a, J. Miret, *et al.*, "Virtual Impedance Loop for Droop-Controlled Single-Phase Parallel Inverters Using a Second-Order General-Integrator Scheme," *Power Electronics, IEEE Transactions on,* vol. 25, pp. 2993-3002, 2010.

[30] L. Xiaonan, S. Kai, J. M. Guerrero, J. C. Vasquez, and H. Lipei, "State-of-Charge Balance Using Adaptive Droop Control for Distributed Energy Storage Systems in DC Microgrid Applications," *Industrial Electronics, IEEE Transactions on,* vol. 61, pp. 2804-2815, 2014.

[31] L. Xiaonan, S. Kai, J. M. Guerrero, J. C. Vasquez, and H. Lipei, "Double-Quadrant State-of-Charge-Based Droop Control Method for Distributed Energy Storage Systems in Autonomous DC Microgrids," *Smart Grid, IEEE Transactions on,* vol. 6, pp. 147-157, 2015.

[32] J. He and Y. W. Li, "Analysis, Design, and Implementation of Virtual Impedance for Power Electronics Interfaced Distributed Generation," *IEEE Transactions on Industry Applications,* vol. 47, pp. 2525-2538, 2011.

[33] J. C. Vasquez, R. A. Mastromauro, J. M. Guerrero, and M. Liserre, "Voltage Support Provided by a Droop-Controlled Multifunctional Inverter," *IEEE Transactions on Industrial Electronics,* vol. 56, pp. 4510-4519, 2009.

Yaser Karimi received the B.S and M.S. degrees in electrical engineering from Sharif University of Technology, Tehran, Iran, in 2008 and 2010, respectively, where he is currently working toward the Ph.D. degree. In 2015, he was a Visiting PhD Student with the Department of Energy Technology, Aalborg University, Aalborg, Denmark. His research interests include power electronics, power converters for renewable energy systems and microgrids.

Hashem Oraee graduated with a First Class Honors degree in Electrical and Electronics Engineering from University of Wales in Cardiff, UK in 1980 and a PhD in Electrical Machines from University of Cambridge, UK in 1984. He is currently a Professor of Electrical Engineering at Sharif University in Iran and the President of Iran Wind Energy Association. His research interests include various aspects of electrical machines, renewable energy and energy economics. He is Fellow of IET and a Senior Member of IEEE.

Mohammad S. Golsorkhi (S'13) received the B.Sc. (Hons.) degree in electrical engineering from Isfahan University of Technology, Isfahan, Iran, in 2009 and the M.Sc. (Hons.) degree in electrical engineering from Tehran Poly-Technique, Tehran, Iran, in 2012. During 2011-2013, he worked in Behrad consulting engineers as a R&D engineer. He is currently pursuing the PhD degree in electrical engineering at The University of Sydney, Australia. In 2015, he was a visiting PhD student with the Department of Energy Technology, Aalborg University, Denmark. His current research interests include control of microgrids, renewable energy resources, and power electronics.

Josep M. Guerrero (S'01-M'04-SM'08-FM'15) received the B.S. degree in telecommunications engineering, the M.S. degree in electronics engineering, and the Ph.D. degree in power electronics, all from the Technical University of Catalonia, Barcelona, Spain, in 1997, 2000, and 2003, respectively.
He was an Associate Professor with the Department of Automatic Control Systems and Computer Engineering, Technical University of Catalonia, Barcelona, Spain. Since 2011, he has been a Full Professor with the Department of Energy Technology, Aalborg University, Aalborg, Denmark, where he is responsible for the microgrid research program. Since 2012, he has also been a Guest Professor with the Chinese Academy of Science and the Nanjing University of Aeronautics and Astronautics.